Long-lived particles and the quiet Sun

R. Andrew Gustafson,[1,*] Ryan Plestid,[2,†] Ian M. Shoemaker,[1,‡] and Albert Zhou[3]

[1]*Center for Neutrino Physics, Department of Physics, Virginia Tech, Blacksburg, Virginia 24061, USA*

[2]*Walter Burke Institute for Theoretical Physics, California Institute of Technology, Pasadena, California 91125, USA*

[3]*Institut für Astroteilchenphysik, Karlsruher Institut für Technologie (KIT), D-76021 Karlsruhe, Germany*

(Received 22 September 2023; accepted 22 December 2023; published 22 January 2024)

The nuclear reaction network within the interior of the Sun is an efficient MeV physics factory and can produce long-lived particles generic to dark sector models. In this work we consider the sensitivity of satellite instruments, primarily the RHESSI spectrometer, that observe the quiet Sun in the MeV regime where backgrounds are low. We find that quiet Sun observations offer a powerful and complementary probe in regions of parameter space, where the long-lived particle decay length is longer than the radius of the Sun and shorter than the distance between the Sun and Earth. We comment on connections to recent model-building work on heavy neutral leptons coupled to neutrinos and high-quality axions from mirror symmetries.

DOI: 10.1103/PhysRevD.109.015020

I. INTRODUCTION

It has long been recognized that the solar interior can serve as an efficient factory for keV-scale physics beyond the Standard Model (BSM), e.g., solar axions and dark photons [1–8]. In addition to thermal production mechanisms, nuclear reactions within the Sun may also source BSM particles up to masses and energies of roughly 15 MeV [4,9–14]. If a flux of long-lived particles (LLPs) in this energy regime emanates from the solar interior, they may transit toward Earth and their decay products can leave detectable signatures. It is important to emphasize that LLPs are generic consequences of a dark sector with relatively light particles and feeble couplings to the Standard Model (SM) [15–18]. As decay lengths become long, LLPs become increasingly difficult to detect and strategies to attack this "lifetime frontier" are valuable tools in the search for BSM physics. This idea has been previously investigated, largely considering FERMI-LAT, in the high energy, i.e., $\gtrsim$100 MeV, regime for annihilating dark matter [19–22].

In this work we point out that existing data from the RHESSI satellite spectrometer [23], which observed the quiet Sun,[1] can place interesting limits on dark sectors with LLPs in the range of $\mathcal{O}(100\ \mathrm{keV})$–$\mathcal{O}(1\ \mathrm{MeV})$. This is an old idea, first proposed by Raffelt and Stodolsky in 1982 in the context of a 200 keV axion [9]; however, it has remained unexplored despite new data in the intervening decades [24]. We illustrate the potential sensitivity of quiet Sun data with a number of BSM examples, emphasizing different production mechanisms that may operate in this mass window. A conservative analysis of existing data from RHESSI is capable of offering complimentary constraints on production mechanisms involving neutrino upscattering and can probe previously untouched regions of parameter space for axionlike particles with masses close to ∼1 MeV. Upcoming missions, such as the COSI satellite [25,26], may be able to substantially improve on the capabilities of RHESSI by (i) taking advantage of a larger instrument surface area, (ii) making use of dead time to carefully study backgrounds, and (iii) taking advantage of distinctive spectral features.

We focus on LLPs that decay primarily to photons[2] and have decay lengths ℓ_{LLP} that satisfy

$$R_\odot \ll \ell_{\mathrm{LLP}} \ll d_\odot, \tag{1}$$

where $R_\odot$ is the radius of the Sun and $d_\odot$ is the distance from the Sun to Earth. This allows an $O(1)$ fraction of the

*gustafr@vt.edu
†rplestid@caltech.edu
‡shoemaker@vt.edu

[1]Time periods without intense surface activity such as solar flares.

[2]We could also consider decays to e^+e^- pairs, but an analysis is complicated by the magnetic fields that surround Earth.

LLPs to decay en route to the satellite instrument. In this limit, the flux of LLPs will never reach any terrestrial experiment since they will decay in flight and their daughter photons will be absorbed in the upper atmosphere. In this sense, quiet Sun observations are complimentary to terrestrial searches for LLPs from the Sun, such as those that have been performed by CAST [10] and Borexino [11].

We perform a straightforward (and conservative) rate-only analysis, the details of which can be found at the end of Sec. II. In the body of the paper, we organize our discussion along the lines of specific BSM scenarios. We discuss neutrino upscattering in Sec. II and solar axion production in Sec. III. We also spend time focusing on model-independent LLP constraints in Sec. IV. In Sec. V we discuss the physics potential for dark sector searches using future missions such as COSI. We close by summarizing our results in Sec. VI.

II. NEUTRINO UPSCATTERING: TRANSITION DIPOLE

We begin by considering a production mechanism involving the upscattering of solar neutrinos transiting through the Sun, e.g., $\nu A \to \mathrm{LLP}A$ with A being a nucleus such as hydrogen or helium (see, e.g., [13,14,27] for results on neutrino upscattering in Earth). This mechanism leverages the large solar neutrino flux, which is copious in the few-hundred keV region and extends up to $\sim$15 MeV. Solar neutrinos have a small probability of being absorbed in the SM because of the small charged current scattering cross section at $E_\nu \sim$ MeV energies. It is, however, possible to have BSM cross sections that exceed the weak interaction at low energies if neutrinos couple via a transition magnetic dipole moment [28,29]. This can lead to sizable conversion probabilities into an unstable right-handed neutrino N (also called a heavy neutral lepton or HNL) for neutrinos transiting from the center to the surface of the Sun. As it is unstable, N may decay in flight, supplying a broad flux of photons in RHESSI. Similar phenomena may occur in the aftermath of SN1987A [30,31] leading to tight limits below the supernova floor derived in [28].

This "dipole portal" can dominate low energy phenomenology since it is a dimension-five operator as compared to the dimension-six contact operator of the weak interaction. Low energy cross sections are then proportional to d^2, with d the dipole moment, vs $G_F^2 E^2$ for weak cross sections. Therefore, dipole portal cross sections can be large at low energies while simultaneously avoiding constraints from higher energy experiments (e.g., accelerator neutrino experiments and colliders). The effective Lagrangian is given by [28]

$$\mathcal{L}_{\mathrm{int}} \supset \sum_\alpha d_\alpha F^{\mu\nu} \bar{N} \sigma_{\mu\nu} P_L \nu_\alpha. \tag{2}$$

Here, d_α represents the coupling between N and each of the three SM neutrinos. In this work, we consider the cases where N couples to a single flavor. This effective interaction has been studied recently in the context of accelerator, solar, atmospheric, and collider neutrinos, as well as in the context of early Universe cosmology and constraints from SN1987A [28,29,32–56].

Unlike the monoenergetic LLP cases discussed later in this paper, the spectrum of E_ν (and hence E_N and E_γ) spans several orders of magnitude. For that reason, we implement a Monte Carlo integration to sample neutrino energy, production location, and upscattering location. We also account for flavor transformation between the three SM neutrino flavors during the neutrino propagation (both due to adiabatic conversion and oscillations).

We consider the Sun to be solely composed of ^{1}H and ^{4}He with densities given by the standard solar model [57–59]. Although larger nuclei would have a cross section that scales as Z^2 due to coherent effects, the relative abundances of these elements are small, so this remains a subdominent effect [58]. Different solar models (i.e., [60]) only differ at the percent level or less, which is a higher level of precision than considered in this paper. All scattering is calculated to be off free nucleons, ignoring the coherent enhancement due to helium. This only leads to an $\sim$10% change in the bounds, which we will see is a much smaller effect than uncertainty in the detector opening angle/background. The cross section for scattering on a free proton is given by $\mathrm{d}\sigma_{\mathrm{dip}} = \mathrm{d}\sigma_1 + \mathrm{d}\sigma_2$, with

$$\frac{\mathrm{d}\sigma_1}{dE_r} = \alpha (2d)^2 F_1^2 \left(\frac{1}{E_r} - \frac{1}{E_\nu} + \frac{m_N^2 (E_r - 2E_\nu - m_p)}{4E_\nu^2 E_r m_p} + \frac{m_N^4 (E_r - m_p)}{8E_\nu^2 E_r^2 m_p^2} \right), \tag{3}$$

and

$$\frac{\mathrm{d}\sigma_2}{dE_r} = \alpha d^2 \mu_n^2 F_2^2 \left[\frac{2m_p}{E_\nu^2} ((2E_\nu - E_r)^2 - 2E_r m_p) + m_N^2 \frac{E_r - 4E_\nu}{E_\nu^2} + \frac{m_N^4}{E_\nu E_r} \right]. \tag{4}$$

Here, F_1 and F_2 are electromagnetic form factors, μ_n is the magnetic moment of the nucleon in question, E_r is the recoil energy, and m_p is the proton mass [61,62]. Since the neutrino energy is much less than the proton mass, the HNL energy E_N is nearly identical to the neutrino energy E_ν. Thus, the flux of HNLs has similar features to the solar neutrino flux (see Fig. 1). Note that, for the parameters considered, the flux of HNLs is $\sim$7 orders of magnitude below the solar neutrino flux, so we do not expect upscattering to have a noticeable effect on solar neutrino detection. The downscattering rate of HNLs will similarly be small, so we do not consider any scattering after production.

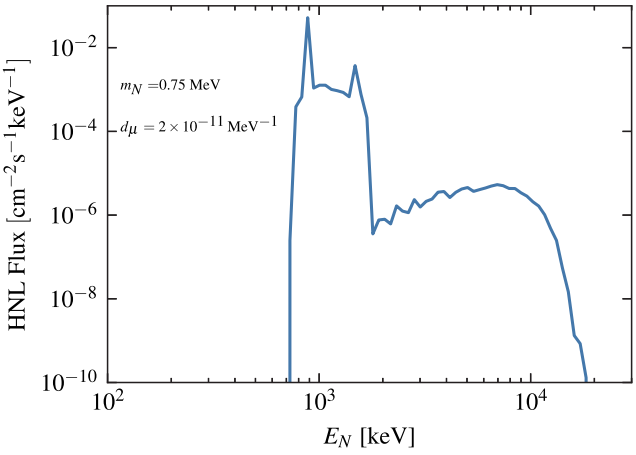

FIG. 1. The flux of solar HNLs at Earth (ignoring decays) as calculated through the dipole model Monte Carlo simulation, where $m_N = 0.75$ MeV and $d_\mu = 2 \times 10^{-11}$ MeV^{-1}.

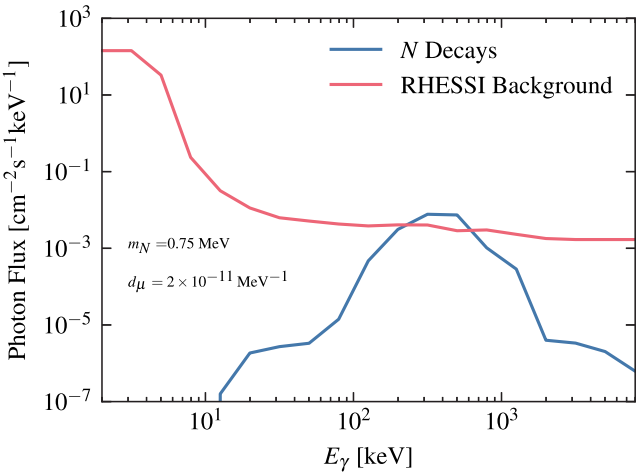

FIG. 2. The flux of photons at RHESSI from N decays calculated using a Monte Carlo integration with a 90° opening angle, compared with the RHESSI background in the front segment. Since the flux from decays exceeds the background, we consider $m_N = 0.75$ MeV, $d_\mu = 2\times10^{-11}$ MeV^{-1} to be excluded.

The HNL has decay channels $N \to \nu_\alpha\gamma$. We consider the ν to be massless and the decays to be isotropic in the rest frame of the HNL.[3] Using the relativistic quantities $\gamma = E_N/m_N$ and $\beta = \sqrt{1 - m_N^2/E_N^2}$, the decay length is calculated as

$$\lambda = \frac{4\pi}{d_\alpha^2 m_N^3}\gamma\beta. \tag{5}$$

The Monte Carlo simulation samples locations for N decays, along with the energy and direction of the decay photon. This is used to calculate the resulting photon flux with respect to energy and angle observed by RHESSI. We consider opening angles for HNL decay photons of 1° and 90°, where we reject all photons arriving at larger angles. The true opening angle is expected to be an energy-dependent value between these two angles, but a full analysis is beyond the scope of this paper. The background flux observed by RHESSI is calculated by using the reported number of counts and effective area of the front segment (ignoring narrow peaks) [23]. We reject a parameter point if the flux from N decays exceeds the observed flux at any energy (see Fig. 2). RHESSI has a good energy resolution (3 keV FWHM at energies below 1 MeV and similar resolutions at higher energies), so we expect the effect to be noticeable even if the BSM photon flux only exceeds the background flux for a small range of energies.

Our resulting exclusion curves from the RHESSI data are shown in Fig. 3 for a muon neutrino dipole coupling. We find that RHESSI data can offer a complimentary (and direct) probe of regions of parameter space that are already probed by SN1987A. Constraints are strongest in the low mass region (sub-MeV), and this may also be probed using coherent elastic neutrino nucleus scattering. We see that the exclusions for the three neutrino flavors all have similar values in Fig. 4. Although the solar neutrino energy extends to ∼15 MeV, the bounds end near $m_N = 1$ MeV. Beyond this mass, the decay length becomes significantly smaller than the radius of the Sun [as can be seen in Eq. (5)], so HNLs are unable to escape before decaying.

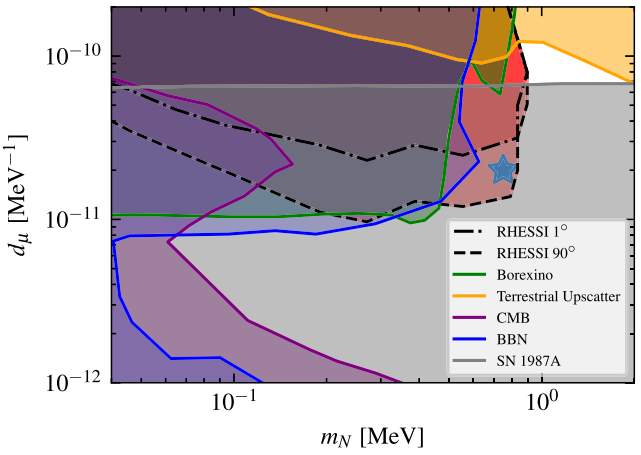

FIG. 3. Excluded parameter space for a muon neutrino transition dipole moment. Along with our bounds, we show 90% C.L. exclusions from Borexino $e-\nu$ scattering [29,64], terrestrial solar neutrino upscattering [14], Supernova (SN) 1987A [28], big bang nucleosynthesis (BBN), and the cosmic microwave background (CMB) [29]. For RHESSI excluded parameter space, we include exclusions from taking a 1° opening angle and a 90° opening angle for photons from HNL decays. For both opening angles, we use the same background. The star represents the parameter point show in Figs. 1 and 2.

[3]In complete generality, the HNL may have some angular correlation with its polarization, but this depends on the details of the model, e.g., Dirac vs Majorana neutrinos [63] and we neglect this in what follows.

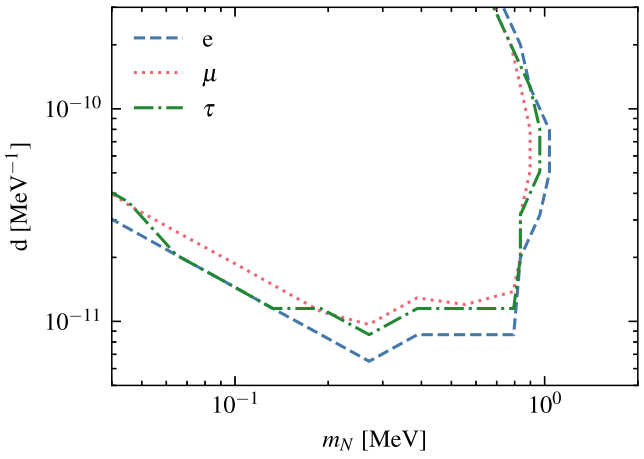

FIG. 4. Excluded parameter space of a transition dipole moment for each of the three active neutrinos. We see that the constraints all take a similar form, only varying by $\mathcal{O}(1)$ factors.

III. HEAVY SOLAR AXIONS

Another production mechanism is solar axions with energies in excess of $E_a \gtrsim 500$ keV. These energies are too high to allow for thermal production (except for in exponentially suppressed tails), and so the background photon fluxes are much smaller than for typically considered keV solar axion searches. The study of MeV-scale solar axions has a long history, and they have been searched for in terrestrial experiments such as Borexino and CAST [10,11]. As we discuss below, satellite measurements of the quiet Sun provide a complimentary probe that excels for decay lengths that are short relative to the Earth-Sun distance.

It is worth highlighting recent work on model building for axions with an extended matter content [65–68]. These models are motivated by the axion quality problem and seek to protect the axion against Planck suppressed corrections. The simplest mechanism to achieve this is to simply break the canonical relation $f_a m_a \approx f_\pi m_\pi$ and to allow for m_a to be "heavy" relative to predictions of conventional (i.e., Dine-Fischler-Srednicki-Zhitnitsky [69,70] or Kim-Shifman-Vainshtein-Zakharov [71,72]) axion models. It is interesting to note that these independent model-building considerations often push the mass and couplings of the axion into regions of parameter space that are well suited for solar axion detection; we will comment on this in great detail below. For instance, following the benchmark scenarios presented in [68], one finds that masses in the ∼10 MeV regime with axion decay constants $f_a \sim 10^{-5}$ GeV^{-1} fall squarely within the "natural" window of parameter space, while simultaneously predicting a sizable coupling to nucleons and a decay length that is a few times longer than the radius of the Sun. For slightly lighter axions, solar production and detection is a useful complimentary probe.

In this section we will parametrize constraints in terms of low energy constants of the effective theory describing axion interactions with nucleons and photons. This may be parametrized by the Lagrangian

$$\mathcal{L}_{\rm int} \subset g_{a\gamma\gamma} F^{\mu\nu}\tilde{F}_{\mu\nu} + \frac{g_{3aN}}{m_N}(\partial_\mu a)\bar{N}\gamma^\mu\tau_3 N. \tag{6}$$

We focus on the isovector coupling because of the $M1$ transition relevant for phenomenology in the Sun. We will allow $g_{a\gamma\gamma}$, the coupling controlling the rate of $a \to \gamma\gamma$, to vary independent of the isovector coupling of axions to nucleons, g_{3aN}. In a UV completion these parameters will be tightly correlated and expressible in terms of the axion decay constant f_a. A reasonable order of magnitude estimate is that $g_{3aN} \sim m_N/f_A$ and $g_{a\gamma\gamma} \sim \frac{\alpha}{4\pi}\frac{1}{f_a}$, however, details are model dependent and we do not discuss them further.

The primary production mechanism for heavy solar axions is the $pd \to {}^3\mathrm{He}\gamma$ reaction, which takes place in the solar pp chain. Other mechanisms are energetically allowed, such as $M1$ transitions in the CNO chain [73] and e^+e^- annihilation from ^{8}B neutrinos in the solar interior, however, we find that the production rates are sufficiently small so as to be uninteresting.

The flux of axions (prior to decay) can be related to the flux of pp neutrinos and depends on the isovector coupling of axions to nucleons g_{3aN} [74]. The axions must first escape the Sun and then decay before reaching Earth. The escape probability depends both on axion absorption and decay processes. Putting all of this together and setting $\mathrm{BR}_{a\gamma\gamma} = 1$, we arrive at the flux of axions arriving at a detector orbiting Earth,

$$\frac{\Phi_\gamma}{\Phi_\nu^{(pp)}} = 0.54|g_{3aN}|^2\left[\frac{p_a}{p_\gamma}\right]^3\left[\mathrm{e}^{-R_\odot/\ell_{\rm abs}} - \mathrm{e}^{-d_\odot/\ell_{\rm dec}}\right], \tag{7}$$

where $\ell_{\rm abs}^{-1} = \ell_{\rm MFP}^{-1} + \ell_{\rm dec}^{-1}$ with $\ell_{\rm MFP}^{-1}$ as the averaged mean free path in the Sun and $\ell_{\rm dec}$ as the axion decay length. The coupling g_{3aN} is the isovector coupling strength of the axion to nucleons, and p_a/p_γ is the ratio of three-momenta between an axion and photon emitted with $E = 5.49$ MeV. The pp neutrino flux is given by $\Phi_\nu^{(pp)} = 6\times10^{10}\,\mathrm{cm}^{-2}\,\mathrm{s}^{-1}$. We account for axion absorption, Primakoff scattering, and axion electron scattering in our calculation of $\ell_{\rm MFP}^{-1}$. The resulting photon flux will be constant in energy over the kinematically allowed photon energies.

Our results are shown in Fig. 5. We note that our exclusions depend on the axion nucleon coupling, captured by g_{3aN}, and the decay constant $g_{a\gamma\gamma}$. If $g_{a\gamma\gamma}$ vanishes at some scale $\mu = \mu_0$, but $g_{aee} \neq 0$, then an effective $g_{a\gamma\gamma} \sim (\alpha/4\pi)g_{aee}/m_e$ will be generated via a one-loop triangle diagram, and in this way one can recast our limits[4] in terms

[4]This requires accounting for the branching ratio to photons, as well as adjusting the decay length.

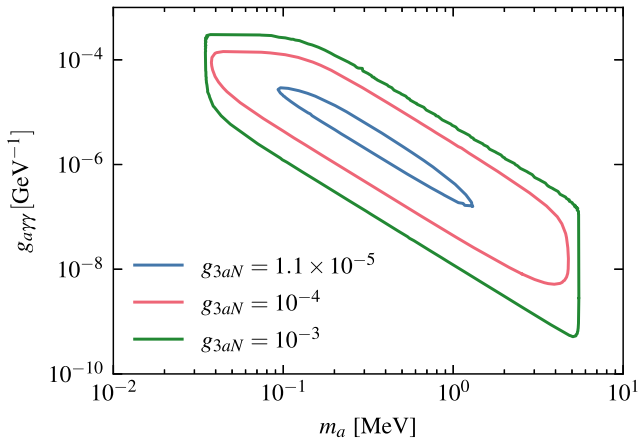

FIG. 5. Contours of g_{3aN} for which the solar axion flux of photons would overwhelm the RHESSI background measurements for the front segments. Sensitivity is exhausted for $g_{3aN} \sim 1 \times 10^{-5}$, however, further reach can be obtained with better data and/or a more sophisticated analysis. To compare with constraints from supernovae [77] and rare kaon decays [79–81], one can use a naive estimate of $g_{3aN} = m_N/f_a$ and $g_{a\gamma\gamma} = \frac{\alpha}{4\pi}\frac{1}{f_a}$, and note that $3 \times 10^4 \lesssim f_a \lesssim 3 \times 10^5$ GeV is allowed by the above constraints (see, e.g., the "conservative" curves in Fig. 9 of Ref. [68]). As an illustration taking $m_a = 1$ MeV and $f_a = 3 \times 10^4$ GeV, one finds $g_{a\gamma\gamma} \sim 2 \times 10^{-8}$ and $g_{3aN} \sim 3 \times 10^{-5}$.

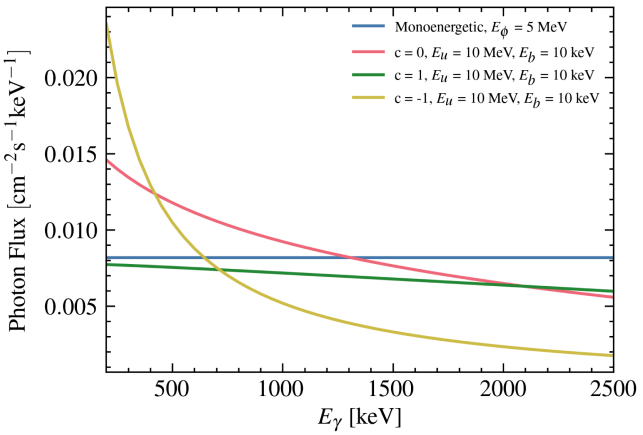

FIG. 6. Comparison of photon fluxes for different ϕ production scenarios. The fluxes are normalized so that the total production rate is $N_\phi = 10^{28}$ s^{-1}, and the decay length is $\lambda = 10R_\odot$ at $E_\phi = 1$ MeV. We consider m_ϕ to be negligibly small.

of those on g_{aee}. We do not include exclusions from SN1987 typically plotted in the m_a-$g_{a\gamma\gamma}$ plane because the values of g_{3aN} that are required to produce a sufficient axion flux in the Sun lead to axion trapping within a core-collapse supernova [75].[5] This is an important distinction between the hadronically coupled axion models we considered here vs an axionlike particle which couples exclusively to photons (see, e.g., [76]). The solar axion constraints we discuss here are therefore complimentary to supernova cooling ones. If the axion nucleon coupling g_{aN} is large enough to evade SN1987 bounds via self trapping, then it is also large enough to be probed with RHESSI data. Low energy supernova observations have been used to place constraints on axions that decay in flight and deposit energy to the ejecta [77]. Additionally, axions produced in neutron star mergers have been constrained using x-ray observation [78]. These constraints also disappear in the strong coupling regime, i.e., for $f_a \lesssim 3 \times 10^5$ GeV, and are complimentary to ours. Constraints from NA62 [79], E787 [80], and E949 [81] are subject to $O(m_K^4/m_\rho^4)$ hadronic uncertainties in the prediction of $K \to a\pi$ [68,82]. These constraints require $f_a \gtrsim 3 \times 10^4$. Finally, our constraints on $g_{a\gamma\gamma}$ lie above the ceiling of searches performed with the Borexino Collaboration [11] because we are sensitive to decay lengths much shorter than $d_\odot$. This is demonstrative of the way in which constraints from solar axions may compliment existing search techniques using accelerator-based experiments, underground detectors, and astrophysical constraints.

Constraints from BBN will generically apply both because the axions we consider have lifetimes in the vicinity of a few seconds and because the same reaction, $pd \to {}^3\mathrm{He}\gamma$, is a key driver of BBN. In the absence of any additional dark sector decay modes, measurements of N_{eff} will generically exclude axions with masses below 5 MeV or so. These constraints can be alleviated if the dark sector contains additional degrees of freedom, see, e.g., [68]. Searches for gamma rays from the quiet Sun offer a complimentary direct probe of axion (or other light particle) production that is independent of early Universe cosmology.

We consider a 90° opening angle for our signal, meaning all decays between the Sun's surface and Earth's orbit contribute. The monoenergetic nature of the axion means the photon flux is constant in energy (see Sec. IV for more details on monoenergetic production). We demand that this flux exceed 1.8×10^{-3} s^{-1} cm^{-2} keV^{-1} for photon energies above 1 MeV so that this flux is above the observed RHESSI background flux in the front segments.

IV. MODEL-INDEPENDENT SEARCHES

We have explored two well-motivated models of long-lived particles which can be probed with RHESSI observations (see the Appendix for other LLP models which are produced too inefficiently to be probed). Let us now consider a model-independent production of LLPs (here called ϕ) which decay via $\phi \to \gamma\gamma$. In this simplified model, we consider all production to occur at the solar center, and ϕ only interacts with SM physics through its decay,

[5]This occurs because axion-nucleon scattering leads to mean free paths much shorter than the typical size of a supernova, trapping the axions.

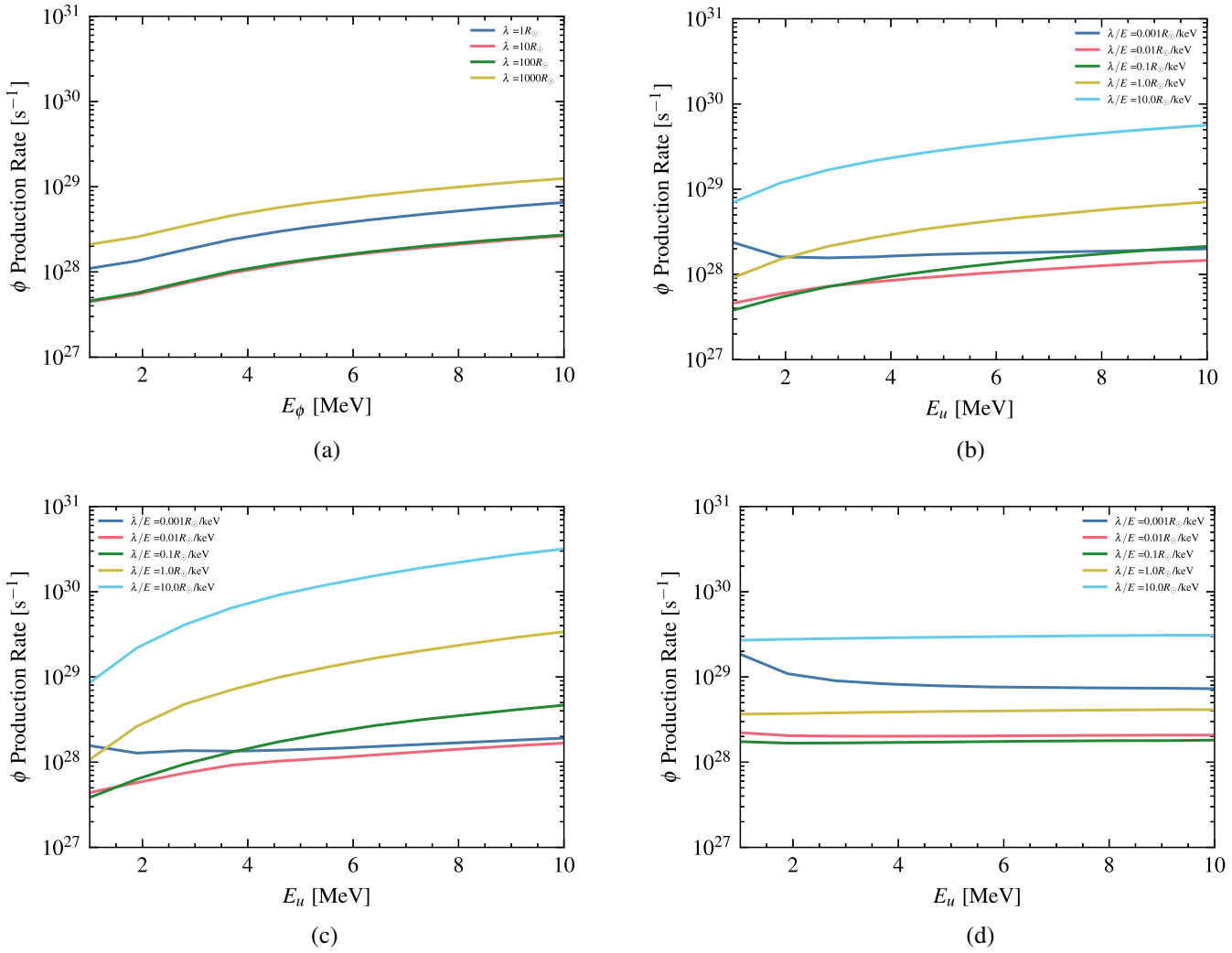

FIG. 7. Exclusion of ϕ production for some of the special cases considered. Production rates above the lines are excluded. In all cases, the mass is considered negligible, and there is no production below 10 keV ($E_b = 10$ keV). (a) Monoenergetic ϕ production; ϕ production (b) uniform in energy ($c = 0$), (c) with a linear dependence on energy ($c = 1$), and (d) inversely proportional to energy ($c = -1$).

so we ignore any possible scattering or absorption. We also assume there is no preferential direction for decay in the rest frame of ϕ, so the flux of photons is a uniform distribution between $E_{\gamma,\min}$ and $E_{\gamma,\max}$, where $E_{\gamma,\max/\min} = 1/2 \times (E_\phi \pm \sqrt{E_\phi^2 - m_\phi^2})$. Inverting this equation, we find $E_\phi \geq E_\gamma + m_\phi^2/(4E_\gamma)$ (we will call this lowest energy $E_{\phi,\min}$). Therefore, if we know the rate of production R_ϕ and decay length λ as a function of E_ϕ, then we can determine the BSM flux of photons at Earth,

$$\frac{d\Phi_\gamma}{dE_\gamma} = \frac{2}{4\pi d_\odot^2} \int_{E_{\phi,\min}}^{\infty} dE_\phi \frac{e^{-R_\odot/\lambda(E_\phi)} - e^{-d_\odot/\lambda(E_\phi)}}{\sqrt{E_\phi^2 - m_\phi^2}} \frac{dR_\phi}{dE_\phi}. \quad (8)$$

One particularly well-motivated morphology is where ϕ has a monoenergetic production spectrum. We have already seen an example of this in the case of monoenergetic axions considered in Sec. III. This would also occur if ϕ is produced via a two-body decay $\chi \to \phi X$ or via annihilation $\chi\chi \to \phi X$ for $v_\chi \ll 1$ and χ and X are some generic particles. Performing the integral in Eq. (8) with a delta-function distribution leads to a flux of photons that is constant in energy between $E_{\gamma,\min}$ and $E_{\gamma,\max}$.

Remaining more agnostic to the source of ϕ production, we may consider a power-law distribution with respect to energy for $E_b \leq E_\phi \leq E_u$,

$$\left.\frac{dR_\phi}{dE_\phi}\right|_{\text{power}} = R_c \times E_\phi^c \Theta(E_u - E_\phi)\Theta(E_\phi - E_b). \quad (9)$$

For $m_\phi \ll E_\gamma, E_\phi$ the photon flux is calculable in closed form,

$$\left.\frac{d\Phi_\gamma}{dE_\gamma}\right|_{\text{power}} = \frac{2R_c}{4\pi d_\odot^2}\left[\left(\frac{R_\odot\tilde{E}}{\tilde{\lambda}}\right)^c\left(\Gamma\left(-c,\frac{R_\odot\tilde{E}}{\tilde{\lambda}E_u}\right)-\Gamma\left(-c,\frac{R_\odot\tilde{E}}{\tilde{\lambda}E_l}\right)\right)-\left(\frac{d_\odot\tilde{E}}{\tilde{\lambda}}\right)^c\left(\Gamma\left(-c,\frac{d_\odot\tilde{E}}{\tilde{\lambda}E_u}\right)-\Gamma\left(-c,\frac{d_\odot\tilde{E}}{\tilde{\lambda}E_l}\right)\right)\right], \quad (10)$$

where $\Gamma(a,x)$ is the incomplete gamma function, $E_l = \max\{E_b, E_{\phi,\min}\}$, and $\tilde{\lambda}$ is the decay length at characteristic energy $\tilde{E}$. We normalize to the total rate of ϕ produced, N_ϕ. For the monoenergetic case, we have $N_\phi = R_\phi$, while for the power-law production, we have

$$R_c = \begin{cases} \frac{N_\phi(c+1)}{E_u^{c+1}-E_b^{c+1}} & \text{for } c \neq -1, \\ \frac{N_\phi}{\log(E_u/E_b)} & \text{for } c = -1. \end{cases} \quad (11)$$

We show example photon fluxes for various values of c in Fig. 6. Constraints on the number of ϕ produced per second in the Sun are shown in Fig. 7. Constraints are set as described at the end of Secs. II and III.

V. FUTURE PROSPECTS

In the above discussion, we have found that repurposing existing RHESSI data is able to provide interesting constraints on light dark sectors with MeV-scale LLPs. Our analysis should be viewed as a proof of principle and certainly underestimates the sensitivity of experiments like RHESSI to new physics models. The major limitations in our analysis are a lack of reliable peak-subtracted spectra and the ability to suppress backgrounds (see [83,84] for recent work in the keV regime for more sophisticated statistical analyses). For example, much of the background for RHESSI comes not from solar activity but rather from cosmic ray interactions with Earth's atmosphere, i.e., the radiation comes from the rear rather than the forward field of view. Much of this background can presumably be suppressed (or perhaps eliminated) with a future instrument, especially if a dedicated search is performed. As our current analysis is systematically limited, an experiment with 10% of RHESSI's background (or with the same background but modeled to a 10% uncertainty) would be 10 times more sensitive to a BSM flux of photons. In what follows, we sketch potential improvements using a near-term MeV telescope. For concreteness we will anchor our discussion around the COSI satellite.[6]

RHESSI operated with minimal shielding to minimize weight. This made the instrument an effectively "all sky" observation with a high level of cosmic ray background activity. In contrast, COSI will operate with active shielding, and its further use of Compton kinematic discrimination offers further background reduction [85]. Moreover, ongoing work to better understand gamma ray emission from the quiet Sun will further improve on irreducible backgrounds [86,87].

Other strategies that could be pursued with a future instrument are to go beyond the rate-only analysis presented above. For example, COSI will have 25% sky coverage and excellent angular resolution. One could image the MeV photon flux differential in both energy and angular position. Depending on the lifetime of LLPs, a "halo" of photons could be searched for outside the solar corona. The shape of the photon distribution will be model dependent, but can be computed using the Monte Carlo simulations outline above. Similarly, taking advantage of COSI's large field of view, other local planetary systems could be used to search for LLPs. This was suggested recently in the context of Jupiter where the capture of light dark matter is better motivated [22,88].

Finally, let us comment on a second channel of interest: LLP $\to e^+e^-$. This may occur for a dark vector that dominantly decays via $V \to e^+e^-$ and has recently been considered (in the context of large volume underground detectors) for the same $pd \to {}^3\text{He}\gamma$ reaction considered here [89]. A search for electrons and/or positrons would require accurate modeling for propagation through magnetic fields in the vicinity of Earth.

VI. CONCLUSIONS AND OUTLOOK

We have discussed simple particle physics models that predict an MeV flux of photons produced by the Sun. The generic requirement is the existence of some LLP that can efficiently transport energy from the interior (fueled by nuclear reactions) to beyond the Sun's surface. Provided the LLP has a sizable branching ratio to final states including at least one photon, e.g., $\gamma\gamma$, $\nu\gamma$, and/or $e^+e^-\gamma$ final states, one can search for energetic gamma rays emanating from the quiet Sun.

We find that constraints from existing data from RHESSI, with a very conservative analysis strategy, can probe small pockets of untouched parameter space for both MeV-scale axions and a neutrino dipole portal. In both cases, the RHESSI analysis provides complimentary coverage to existing search strategies (including cosmological probes such as BBN).

Our major motivation is a simple proof of principle that MeV-scale LLPs with decay lengths larger than the radius of the Sun can be efficiently searched for using solar telescopes. The analysis presented here is conservative and fairly crude; we define exclusions by the condition that the BSM signal prediction exceeds the *total signal* observed in any energy window by RHESSI. Constraints and/or discovery potential could be substantially improved with a better understanding of instrument backgrounds and more

[6]We thank Albert Shih for pointing out the COSI mission to us.

sophisticated analysis techniques. For example, one could make use of angular profiles of incident photons to search for new physics, as an LLP flux will produce a photon flux outside the stellar corona with a predictable angular shape/morphology. We encourage future missions with MeV-scale instrumentation below the cutoff of Fermi-Lat, such as COSI [25,26], to consider searches for BSM particles, with the Sun being a well-motivated engine for MeV-scale LLPs.

ACKNOWLEDGMENTS

This work benefited from feedback at the Simon's Center for Geometry and Physics, and R. P. would like to specifically thank Simon Knapen, Rebecca Leanne, and Jessie Shelton for useful discussions. We thank Albert Shih for helpful discussions regarding the RHESSI instrument. We benefited from feedback on this manuscript from Rebccea Leanne and Elena Pinetti. R. P. is supported by the U.S. Department of Energy, Office of Science, Office of High Energy Physics, under Award No. DE-SC0011632 and by the Walter Burke Institute for Theoretical Physics. R. P. is supported by the Neutrino Theory Network under Grant No. DEAC02-07CHI11359, the U.S. Department of Energy, Office of Science, Office of High Energy Physics, under Award No. DE-SC0011632, and by the Walter Burke Institute for Theoretical Physics. I. M. S. and R. A. G. are supported by the U.S. Department of Energy Office of Science, Office of High Energy Physics, under Award No. DE-SC0020262.

APPENDIX: INEFFICIENT PRODUCTION MECHANISMS

In this appendix, we discuss production mechanisms that we have found to be too inefficient to allow for detection prospects with our RHESSI analysis.

1. Mass-mixing portal for HNLs

Another BSM model involving HNLs has N couple directly to active neutrinos through added elements in the Pontecorvo-Maki-Nakagawa-Sakata matrix [13,48,90–111]. Active neutrinos contain a small admixture of the HNLs along with the three known mass states,

$$\nu_\alpha = U_{\alpha N} N + \sum_{i=1}^{3} U_{\alpha i} \nu_i, \tag{A1}$$

where $U_{\alpha N}$ represents the coupling of HNLs to active neutrinos. Since the Sun only has nuclear reactions that produce electron neutrinos, our constraint is on U_{eN}. The N flux from upscattering is subdominant by orders of magnitude to that from direct production. Therefore, the flux is given by rescaling the neutrino flux,

$$\Phi_N = |U_{Ne}|^2 \Phi_\nu \sqrt{1 - m_N^2/E_N^2}. \tag{A2}$$

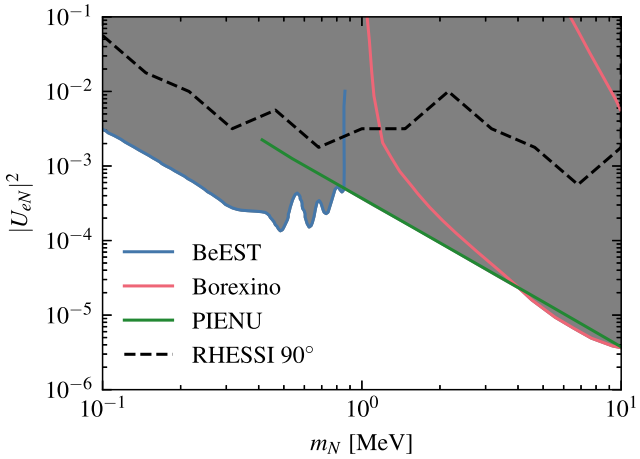

FIG. 8. Excluded parameter space for HNLs in the mass-mixing model. The dashed line shows the RHESSI exclusion, while shaded regions come from BeEST [90], PIENU [91], and Borexino [92].

For the masses considered here, there are only three decay channels: (i) $N \to 3\nu$, (ii) $N \to \nu\gamma$, and (iii) $N \to \nu e^+ e^-$. As with other production mechanisms, we only consider signals from photons. The geometry of this decay (into a massless neutrino and photon) is identical to the case of the dipole portal. The decay rate for each of the processes follows the general form

$$\Gamma_{N\to SM} \propto G_F^2 |U_{eN}|^2 m_N^5, \tag{A3}$$

which has the steep power-law dependence on mass typical of weak decays. We find that, since decay lengths are always long enough to fall outside the range given in Eq. (1), sensitivity from RHESSI is subdominant to searches at Borexino (which benefits from a large detector volume) and from direct laboratory searches (see Fig. 8).

2. Captured dark matter in the Sun

If heavy dark matter χ has interactions beyond gravity, it may scatter within large celestial bodies and become gravitationally captured. The Sun, being by far the most massive object in the solar system, is a strong candidate in searching for the signals from captured χ [21,112–128].

For the case of symmetric dark matter with a long-lived particle mediator, there is the interaction $\chi\bar{\chi} \to$ LLPs. The energies of these final observable particles are $\mathcal{O}(m_\chi)$. However, as discussed in [115], for thermal relic annihilation cross sections, short range interactions with SM, and m_χ below a few GeV, most of the χ evaporates from the Sun before annihilating. Even Jupiter, which has a cooler core than the Sun, would have evaporation be the dominant effect for $m_\chi \leq 0.7$ GeV [129], far above the energy sensitivity of RHESSI. We note that, in the presence of long-range $\chi -$ SM interactions, evaporation may be suppressed [22,88]. However, this is a model-dependent scenario and is not considered in this work.

We also considered the case of asymmetric dark matter with self-interactions via a scalar ϕ with a Yukawa-like interaction $\mathcal{L} \subset \bar{\chi}\chi\phi$. As there is no annihilation, in the absence of evaporation, the χ population grows indefinitely. Virialized dark matter passing through the Sun can scatter on the trapped overdensity and produce LLPs via the bremsstrahlunglike reaction $\chi\chi \to \chi\chi\phi$. In order to produce MeV gamma rays, we require heavy dark matter, $m_\chi \gtrsim 1$ TeV, such that there is sufficient available kinetic energy $m_\chi v_\chi^2 \gtrsim 1$ MeV.[7] In order to produce a sufficiently large flux of LLPs, we require a sizable $\chi\chi \to \chi\chi$ cross section. This can only be achieved with a light mediator for TeV-scale (or heavier) dark matter. The cross section relies on a small momentum transfers. Nonrelativistic kinematics, however, demand a parametrically larger momentum transfer in the bremsstrahlunglike reaction than for elastic scattering. For example, demanding $E_\phi \sim \mathcal{O}(\mathrm{MeV})$ bremsstrahlung, requires a momentum transfer on the order of $\Delta p^2 \sim m_\chi E_\phi \sim (1\ \mathrm{GeV})^2$. Because of this kinematic suppression, we find that RHESSI is incapable of setting competitive limits even with the most generous/optimistic model-building choices to maximize the bremsstrahlung-like cross section.

[7]Dark matter nucleon scattering cannot induce MeV bremsstrahlung (i.e., via $\chi N \to \chi N\phi$), because the available kinetic energy is set by $m_N v_\chi^2 \sim 1\ \mathrm{keV} \times (v_\chi/10^{-3})^2$. This is most easily seen in the rest frame of the heavy dark matter.

[1] P. Sikivie, Experimental tests of the invisible axion, Phys. Rev. Lett. **51**, 1415 (1983); **52**, 695(E) (1984).

[2] Savas Dimopoulos, Joshua A. Frieman, B. W. Lynn, and G. D. Starkman, Axiorecombination: A new mechanism for stellar axion production, Phys. Lett. B **179**, 223 (1986).

[3] F. T. Avignone III, R. L. Brodzinski, S. Dimopoulos, G. D. Starkman, A. K. Drukier, D. N. Spergel, G. Gelmini, and B. W. Lynn, Laboratory limits on solar axions from an ultralow background germanium spectrometer, Phys. Rev. D **35**, 2752 (1987).

[4] Georg G. Raffelt, Astrophysical methods to constrain axions and other novel particle phenomena, Phys. Rep. **198**, 1 (1990).

[5] Remy Battesti, Berta Beltran, Hooman Davoudiasl, Markus Kuster, Pierre Pugnat, Raul Rabadan, Andreas Ringwald, Neil Spooner, and Konstantin Zioutas, Axion searches in the past, at present, and in the near future, Lect. Notes Phys. **741**, 199 (2008).

[6] Maxim Pospelov, Adam Ritz, and Mikhail B. Voloshin, Bosonic super-WIMPs as keV-scale dark matter, Phys. Rev. D **78**, 115012 (2008).

[7] Haipeng An, Maxim Pospelov, Josef Pradler, and Adam Ritz, Direct detection constraints on dark photon dark matter, Phys. Lett. B **747**, 331 (2015).

[8] Peter W. Graham, Igor G. Irastorza, Steven K. Lamoreaux, Axel Lindner, and Karl A. van Bibber, Experimental searches for the axion and axion-like particles, Annu. Rev. Nucl. Part. Sci. **65**, 485 (2015).

[9] Georg Raffelt and Leo Stodolsky, New particles from nuclear reactions in the Sun, Phys. Lett. B **119**, 323 (1982).

[10] S. Andriamonje *et al.* (CAST Collaboration), Search for solar axion emission from ^{7}Li and D$(p,\gamma)^3$He nuclear decays with the CAST γ-ray calorimeter, J. Cosmol. Astropart. Phys. 03 (2010) 032.

[11] G. Bellini *et al.* (Borexino Collaboration), Search for solar axions produced in $p(d,{}^3\mathrm{He})A$ reaction with Borexino detector, Phys. Rev. D **85**, 092003 (2012).

[12] G. Bellini *et al.* (Borexino Collaboration), New limits on heavy sterile neutrino mixing in B8 decay obtained with the Borexino detector, Phys. Rev. D **88**, 072010 (2013).

[13] Ryan Plestid, Luminous solar neutrinos II: Mass-mixing portals, Phys. Rev. D **104**, 075028 (2021); **105**, 099901(E) (2022).

[14] Ryan Plestid, Luminous solar neutrinos I: Dipole portals, Phys. Rev. D **104**, 075027 (2021).

[15] J. Beacham *et al.*, Physics beyond colliders at CERN: Beyond the standard model working group report, J. Phys. G **47**, 010501 (2020).

[16] Prateek Agrawal *et al.*, Feebly-interacting particles: FIPs 2020 workshop report, Eur. Phys. J. C **81**, 1015 (2021).

[17] David Curtin *et al.*, Long-lived particles at the energy frontier: The MATHUSLA physics case, Rep. Prog. Phys. **82**, 116201 (2019).

[18] Simon Knapen and Steven Lowette, A guide to hunting long-lived particles at the LHC, arXiv:2212.03883.

[19] Philip Schuster, Natalia Toro, and Itay Yavin, Terrestrial and solar limits on long-lived particles in a dark sector, Phys. Rev. D **81**, 016002 (2010).

[20] Brian Batell, Maxim Pospelov, Adam Ritz, and Yanwen Shang, Solar gamma rays powered by secluded dark matter, Phys. Rev. D **81**, 075004 (2010).

[21] Rebecca K. Leane, Kenny C. Y. Ng, and John F. Beacom, Powerful solar signatures of long-lived dark mediators, Phys. Rev. D **95**, 123016 (2017).

[22] Rebecca K. Leane and Tim Linden, First analysis of Jupiter in gamma rays and a new search for dark matter, Phys. Rev. Lett. **131**, 071001 (2023).

[23] David M. Smith, R. P. Lin, P. Turin, D. W. Curtis, J. H. Primbsch, R. D. Campbell, R. Abiad, P. Schroeder, C. P. Cork, E. L. Hull *et al.*, The RHESSI spectrometer, in *The Reuven Ramaty High-Energy Solar Spectroscopic Imager (RHESSI)* (Springer, Dordrecht, 2003).

[24] Brian R. Dennis, Albert Y. Shih, Gordon J. Hurford, and Pascal Saint-Hilaire, Ramaty High Energy Solar

Spectroscopic Imager (RHESSI), in *Handbook of X-Ray and Gamma-Ray Astrophysics*, edited C. Bambi and A. Santangelo (Springer, Singapore, 2022), 10.1007/978-981-16-4544-0_169-1.
[25] COSI Team, COSI, https://cosi.ssl.berkeley.edu/.
[26] John A. Tomsick (COSI Team), The Compton spectrometer and imager project for MeV astronomy, Proc. Sci. ICRC2021 (**2021**) 652 [arXiv:2109.10403].
[27] R. Andrew Gustafson, Ryan Plestid, and Ian M. Shoemaker, Neutrino portals, terrestrial upscattering, and atmospheric neutrinos, Phys. Rev. D **106**, 095037 (2022).
[28] Gabriel Magill, Ryan Plestid, Maxim Pospelov, and Yu-Dai Tsai, Dipole portal to heavy neutral leptons, Phys. Rev. D **98**, 115015 (2018).
[29] Vedran Brdar, Admir Greljo, Joachim Kopp, and Toby Opferkuch, The neutrino magnetic moment portal: Cosmology, astrophysics, and direct detection, J. Cosmol. Astropart. Phys. 01 (2021) 039.
[30] Vedran Brdar, André de Gouvêa, Ying-Ying Li, and Pedro A. N. Machado, The neutrino magnetic moment portal and supernovae: New constraints and multimessenger opportunities, Phys. Rev. D **107**, 073005 (2023).
[31] Matheus Hostert and Maxim Pospelov (private communication).
[32] S. N. Gninenko, The MiniBooNE anomaly and heavy neutrino decay, Phys. Rev. Lett. **103**, 241802 (2009).
[33] Sergei N. Gninenko, A resolution of puzzles from the LSND, KARMEN, and MiniBooNE experiments, Phys. Rev. D **83**, 015015 (2011).
[34] David McKeen and Maxim Pospelov, Muon capture constraints on sterile neutrino properties, Phys. Rev. D **82**, 113018 (2010).
[35] Manuel Masip and Pere Masjuan, Heavy-neutrino decays at neutrino telescopes, Phys. Rev. D **83**, 091301 (2011).
[36] Manuel Masip, Pere Masjuan, and Davide Meloni, Heavy neutrino decays at MiniBooNE, J. High Energy Phys. 01 (2013) 106.
[37] Pilar Coloma, Pedro A. N. Machado, Ivan Martinez-Soler, and Ian M. Shoemaker, Double-cascade events from new physics in IceCube, Phys. Rev. Lett. **119**, 201804 (2017).
[38] Ian M. Shoemaker and Jason Wyenberg, Direct detection experiments at the neutrino dipole portal frontier, Phys. Rev. D **99**, 075010 (2019).
[39] Carlos A. Argüelles, Matheus Hostert, and Yu-Dai Tsai, Testing new physics explanations of the MiniBooNE anomaly at neutrino scattering experiments, Phys. Rev. Lett. **123**, 261801 (2019).
[40] Matheus. Hostert, Hidden physics at the neutrino frontier: Tridents, dark forces, and hidden particles, Ph.D. thesis, Durham University, 2019.
[41] Oliver Fischer, Álvaro Hernández-Cabezudo, and Thomas Schwetz, Explaining the MiniBooNE excess by a decaying sterile neutrino with mass in the 250 MeV range, Phys. Rev. D **101**, 075045 (2020).
[42] Pilar Coloma, Pilar Hernández, Víctor Muñoz, and Ian M. Shoemaker, New constraints on heavy neutral leptons from Super-Kamiokande data, Eur. Phys. J. C **80**, 235 (2020).
[43] Thomas Schwetz, Albert Zhou, and Jing-Yu Zhu, Constraining active-sterile neutrino transition magnetic moments at DUNE near and far detectors, J. High Energy Phys. 07 (2020) 200.
[44] Chiara Arina, Andrew Cheek, Ken Mimasu, and Luca Pagani, Light and darkness: Consistently coupling dark matter to photons via effective operators, Eur. Phys. J. C **81**, 223 (2021).
[45] Ian M. Shoemaker, Yu-Dai Tsai, and Jason Wyenberg, Active-to-sterile neutrino dipole portal and the XENON1T excess, Phys. Rev. D **104**, 115026 (2021).
[46] Asli Abdullahi, Matheus Hostert, and Silvia Pascoli, A dark seesaw solution to low energy anomalies: MiniBooNE, the muon $(g-2)$, and *BABAR*, Phys. Lett. B **820**, 136531 (2021).
[47] Soroush Shakeri, Fazlollah Hajkarim, and She-Sheng Xue, Shedding new light on sterile neutrinos from XENON1T experiment, J. High Energy Phys. 12 (2020) 194.
[48] Mack Atkinson, Pilar Coloma, Ivan Martinez-Soler, Noemi Rocco, and Ian M. Shoemaker, Heavy neutrino searches through double-bang events at Super-Kamiokande, DUNE, and Hyper-Kamiokande, J. High Energy Phys. 04 (2022) 174.
[49] Wonsub Cho, Ki-Young Choi, and Osamu Seto, Sterile neutrino dark matter with dipole interaction, Phys. Rev. D **105**, 015016 (2022).
[50] Jihn E. Kim, Arnab Dasgupta, and Sin Kyu Kang, Probing neutrino dipole portal at COHERENT experiment, J. High Energy Phys. 11 (2021) 120.
[51] Carlos A. Argüelles, Nicolò Foppiani, and Matheus Hostert, Heavy neutral leptons below the kaon mass at hodoscopic detectors, Phys. Rev. D **105**, 095006 (2022).
[52] Ahmed Ismail, Sudip Jana, and Roshan Mammen Abraham, Neutrino up-scattering via the dipole portal at forward LHC detectors, Phys. Rev. D **105**, 055008 (2022).
[53] O. G. Miranda, D. K. Papoulias, O. Sanders, M. Tórtola, and J. W. F. Valle, Low-energy probes of sterile neutrino transition magnetic moments, J. High Energy Phys. 12 (2021) 191.
[54] Patrick D. Bolton, Frank F. Deppisch, Kåre Fridell, Julia Harz, Chandan Hati, and Suchita Kulkarni, Probing active-sterile neutrino transition magnetic moments with photon emission from CEνNS, Phys. Rev. D **106**, 035036 (2022).
[55] Krzysztof Jodłowski and Sebastian Trojanowski, Neutrino beam-dump experiment with FASER at the LHC, J. High Energy Phys. 05 (2021) 191.
[56] Stefano Vergani, Nicholas W. Kamp, Alejandro Diaz, Carlos A. Argüelles, Janet M. Conrad, Michael H. Shaevitz, and Melissa A. Uchida, Explaining the MiniBooNE excess through a mixed model of neutrino oscillation and decay, Phys. Rev. D **104**, 095005 (2021).
[57] John N. Bahcall and M. H. Pinsonneault, What do we (not) know theoretically about solar neutrino fluxes?, Phys. Rev. Lett. **92**, 121301 (2004).
[58] John N. Bahcall, Aldo M. Serenelli, and Sarbani Basu, 10,000 standard solar models: A Monte Carlo simulation, Astrophys. J. Suppl. Ser. **165**, 400 (2006).
[59] John Bahcall, Standard solar model, http://www.sns.ias.edu/ jnb/SNdata/sndata.html#bs2005.
[60] Núria Vinyoles, Aldo M. Serenelli, Francesco L. Villante, Sarbani Basu, Johannes Bergström, M. C. Gonzalez-Garcia, Michele Maltoni, Carlos Peña-Garay, and Ningqiang Song,

A new generation of standard solar models, Astrophys. J. **835**, 202 (2017).
[61] Kaushik Borah, Richard J. Hill, Gabriel Lee, and Oleksandr Tomalak, Parametrization and applications of the low-Q^2 nucleon vector form factors, Phys. Rev. D **102**, 074012 (2020).
[62] J. Arrington, Implications of the discrepancy between proton form factor measurements, Phys. Rev. C **69**, 022201 (2004).
[63] A. Baha Balantekin, André de Gouvêa, and Boris Kayser, Addressing the Majorana vs. Dirac question with neutrino decays, Phys. Lett. B **789**, 488 (2019).
[64] Borexino Collaboration, Comprehensive measurement of pp-chain solar neutrinos, Nature (London) **562**, 505 (2018).
[65] Hajime Fukuda, Keisuke Harigaya, Masahiro Ibe, and Tsutomu T. Yanagida, Model of visible QCD axion, Phys. Rev. D **92**, 015021 (2015).
[66] Prateek Agrawal and Kiel Howe, Factoring the strong CP problem, J. High Energy Phys. 12 (2018) 029.
[67] Anson Hook, Soubhik Kumar, Zhen Liu, and Raman Sundrum, High quality QCD axion and the LHC, Phys. Rev. Lett. **124**, 221801 (2020).
[68] David I. Dunsky, Lawrence J. Hall, and Keisuke Harigaya, A heavy QCD axion and the mirror world, arXiv: 2302.04274.
[69] Michael Dine, Willy Fischler, and Mark Srednicki, A simple solution to the strong CP problem with a harmless axion, Phys. Lett. B **104**, 199 (1981).
[70] A. R. Zhitnitsky, On possible suppression of the axion hadron interactions. (In Russian), Sov. J. Nucl. Phys. **31**, 260 (1980), https://inspirehep.net/literature/157263.
[71] Jihn E. Kim, Weak interaction singlet and strong CP invariance, Phys. Rev. Lett. **43**, 103 (1979).
[72] Mikhail A. Shifman, A. I. Vainshtein, and Valentin I. Zakharov, Can confinement ensure natural CP invariance of strong interactions?, Nucl. Phys. **B166**, 493 (1980).
[73] R. Massarczyk, P. H. Chu, and S. R. Elliott, Axion emission from nuclear magnetic dipole transitions, Phys. Rev. D **105**, 015031 (2022).
[74] T. W. Donnelly, S. J. Freedman, R. S. Lytel, R. D. Peccei, and M. Schwartz, Do axions exist?, Phys. Rev. D **18**, 1607 (1978).
[75] Jae Hyeok Chang, Rouven Essig, and Samuel D. McDermott, Supernova 1987A constraints on sub-GeV dark sectors, millicharged particles, the QCD axion, and an axion-like particle, J. High Energy Phys. 09 (2018) 051.
[76] Joerg Jaeckel and Michael Spannowsky, Probing MeV to 90 GeV axion-like particles with LEP and LHC, Phys. Lett. B **753**, 482 (2016).
[77] Andrea Caputo, Hans-Thomas Janka, Georg Raffelt, and Edoardo Vitagliano, Low-energy supernovae severely constrain radiative particle decays, Phys. Rev. Lett. **128**, 221103 (2022).
[78] Melissa Diamond, Damiano FG Fiorillo, Gustavo Marques-Tavares, Irene Tamborra, and Edoardo Vitagliano, Multi-messenger constraints on radiatively decaying axions from GW170817, arXiv:2305.10327.
[79] Eduardo Cortina Gil *et al.* (NA62 Collaboration), Measurement of the very rare K^+ $\pi^+\nu\bar{\nu}$ decay, J. High Energy Phys. 06 (2021) 093.
[80] S. Adler *et al.* (E787 Collaboration), Further search for the decay $K^+ \to \pi^+\nu\bar{\nu}$ in the momentum region $P < 195\ \mathrm{MeV}/c$, Phys. Rev. D **70**, 037102 (2004).
[81] A. V. Artamonov *et al.* (BNL-E949 Collaboration), Study of the decay $K^+ \to \pi^+\nu\bar{\nu}$ in the momentum region $140 < P_\pi < 199\ \mathrm{MeV}/c$, Phys. Rev. D **79**, 092004 (2009).
[82] Martin Bauer, Matthias Neubert, Sophie Renner, Marvin Schnubel, and Andrea Thamm, Consistent treatment of axions in the weak chiral Lagrangian, Phys. Rev. Lett. **127**, 081803 (2021).
[83] William DeRocco, Shalma Wegsman, Brian Grefenstette, Junwu Huang, and Ken Van Tilburg, First indirect detection constraints on axions in the solar basin, Phys. Rev. Lett. **129**, 101101 (2022).
[84] Jonas Frerick, Felix Kahlhoefer, and Kai Schmidt-Hoberg, A' view of the sunrise: Boosting helioscopes with angular information, J. Cosmol. Astropart. Phys. 03 (2023) 001.
[85] S. E. Boggs and P. Jean, Event reconstruction in high resolution Compton telescopes, Astron. Astrophys. Suppl. Ser. **145**, 311 (2000).
[86] Elena Orlando and Andrew Strong, StellarICS: Inverse Compton emission from the quiet Sun and stars from keV to TeV, J. Cosmol. Astropart. Phys. 04 (2021) 004.
[87] Elena Orlando, Vahe' Petrosian, and Andrew Strong, A new component from the quiet Sun from radio to gamma rays: Synchrotron radiation by galactic cosmic-ray electrons, Astrophys. J. **943**, 173 (2023).
[88] Javier F. Acevedo, Rebecca K. Leane, and Juri Smirnov, Evaporation barrier for dark matter in celestial bodies, arXiv:2303.01516.
[89] Francesco D'Eramo, Giuseppe Lucente, Newton Nath, and Seokhoon Yun, Terrestrial detection of hidden vectors produced by solar nuclear reactions, J. High Energy Phys. 12 (2023) 091.
[90] S. Friedrich, G. B. Kim, C. Bray, R. Cantor, J. Dilling, S. Fretwell, J. A. Hall, A. Lennarz, V. Lordi, P. Machule *et al.*, Limits on the existence of sub-MeV sterile neutrinos from the decay of Be^7 in superconducting quantum sensors, Phys. Rev. Lett. **126**, 021803 (2021).
[91] D. A. Bryman and R. Shrock, Improved constraints on sterile neutrinos in the MeV to GeV mass range, Phys. Rev. D **100**, 053006 (2019).
[92] G. Bellini, J. Benziger, D. Bick, G. Bonfini, D. Bravo, M. Buizza Avanzini, B. Caccianiga, L. Cadonati, F. Calaprice, P. Cavalcante *et al.*, New limits on heavy sterile neutrino mixing in B^8 decay obtained with the Borexino detector, Phys. Rev. D **88**, 072010 (2013).
[93] Carlos Argüelles, Pilar Coloma, Pilar Hernández, and Víctor Muñoz, Searches for atmospheric long-lived particles, J. High Energy Phys. 02 (2020) 190.
[94] D. Liventsev *et al.* (Belle Collaboration), Search for heavy neutrinos at Belle, Phys. Rev. D **87**, 071102 (2013); **95**, 099903(E) (2017).
[95] Takehiko Asaka and Mikhail Shaposhnikov, The νMSM, dark matter and baryon asymmetry of the Universe, Phys. Lett. B **620**, 17 (2005).
[96] Takehiko Asaka, Steve Blanchet, and Mikhail Shaposhnikov, The νMSM, dark matter and neutrino masses, Phys. Lett. B **631**, 151 (2005).

[97] Anupama Atre, Tao Han, Silvia Pascoli, and Bin Zhang, The search for heavy Majorana neutrinos, J. High Energy Phys. 05 (2009) 030.
[98] Loretta M. Johnson, Douglas W. McKay, and Tim Bolton, Extending sensitivity for low mass neutral heavy lepton searches, Phys. Rev. D **56**, 2970 (1997).
[99] Jean-Michel Levy (T2K Collaboration), Rates and differential distributions in heavy neutral leptons production and decays, arXiv:1805.06419.
[100] Joseph A. Formaggio, Janet M. Conrad, Michael Shaevitz, Artur Vaitaitis, and Robert Drucker, Helicity effects in neutral heavy lepton decays, Phys. Rev. D **57**, 7037 (1998).
[101] Dmitry Gorbunov and Mikhail Shaposhnikov, How to find neutral leptons of the νMSM?, J. High Energy Phys. 10 (2007) 015; 11 (2013) 101(E).
[102] Marco Drewes, The phenomenology of right handed neutrinos, Int. J. Mod. Phys. E **22**, 1330019 (2013).
[103] Kyrylo Bondarenko, Alexey Boyarsky, Dmitry Gorbunov, and Oleg Ruchayskiy, Phenomenology of GeV-scale heavy neutral leptons, J. High Energy Phys. 11 (2018) 032.
[104] Alexey Boyarsky, Oleg Ruchayskiy, and Mikhail Shaposhnikov, The role of sterile neutrinos in cosmology and astrophysics, Annu. Rev. Nucl. Part. Sci. **59**, 191 (2009).
[105] Jeffrey M. Berryman, Andre de Gouvea, Patrick J. Fox, Boris Jules Kayser, Kevin James Kelly, and Jennifer Lynne Raaf, Searches for decays of new particles in the DUNE multi-purpose near detector, J. High Energy Phys. 02 (2020) 174.
[106] Peter Ballett, Tommaso Boschi, and Silvia Pascoli, Heavy neutral leptons from low-scale seesaws at the DUNE near detector, J. High Energy Phys. 03 (2020) 111.
[107] Graciela B. Gelmini, Alexander Kusenko, and Volodymyr Takhistov, Possible hints of sterile neutrinos in recent measurements of the Hubble parameter, J. Cosmol. Astropart. Phys. 06 (2021) 002.
[108] J. Orloff, Alexandre N. Rozanov, and C. Santoni, Limits on the mixing of tau neutrino to heavy neutrinos, Phys. Lett. B **550**, 8 (2002).
[109] Iryna Boiarska, Alexey Boyarsky, Oleksii Mikulenko, and Maksym Ovchynnikov, Constraints from the CHARM experiment on heavy neutral leptons with tau mixing, Phys. Rev. D **104**, 095019 (2021).
[110] Nashwan Sabti, Andrii Magalich, and Anastasiia Filimonova, An extended analysis of heavy neutral leptons during big bang nucleosynthesis, J. Cosmol. Astropart. Phys. 11 (2020) 056.
[111] R. Acciarri, C. Adams, J. Asaadi, B. Baller, V. Basque, F. Cavanna, A. de Gouvêa, R. S. Fitzpatrick, B. Fleming, P. Green, C. James, K. J. Kelly, I. Lepetic, X. Luo, O. Palamara, G. Scanavini, M. Soderberg, J. Spitz, A. M. Szelc, W. Wu, and T. Yang (ArgoNeuT Collaboration), New constraints on tau-coupled heavy neutral leptons with masses $m_N =$ 280–970 MeV, Phys. Rev. Lett. **127**, 121801 (2021).
[112] William H. Press and David N. Spergel, Capture by the Sun of a galactic population of weakly interacting massive particles, Astrophys. J. **296**, 679 (1985).
[113] Andrew Gould, WIMP distribution in and evaporation from the Sun, Astrophys. J. **321**, 560 (1987).
[114] Andrew Gould, Resonant enhancements in weakly interacting massive particle capture by the Earth, Astrophys. J. **321**, 571 (1987).
[115] Raghuveer Garani and Sergio Palomares-Ruiz, Dark matter in the Sun: Scattering off electrons vs nucleons, J. Cosmol. Astropart. Phys. 05 (2017) 007.
[116] Mads T Frandsen and Subir Sarkar, Asymmetric dark matter and the Sun, Phys. Rev. Lett. **105**, 011301 (2010).
[117] Philip Schuster, Natalia Toro, Neal Weiner, and Itay Yavin, High energy electron signals from dark matter annihilation in the Sun, Phys. Rev. D **82**, 115012 (2010).
[118] Nicole F. Bell and Kalliopi Petraki, Enhanced neutrino signals from dark matter annihilation in the Sun via metastable mediators, J. Cosmol. Astropart. Phys. 04 (2011) 003.
[119] Jonathan L. Feng, Jordan Smolinsky, and Philip Tanedo, Detecting dark matter through dark photons from the Sun: Charged particle signatures, Phys. Rev. D **93**, 115036 (2016).
[120] Rouzbeh Allahverdi, Yu Gao, Bradley Knockel, and Shashank Shalgar, Indirect signals from solar dark matter annihilation to long-lived right-handed neutrinos, Phys. Rev. D **95**, 075001 (2017).
[121] Chiara Arina, Mihailo Backović, Jan Heisig, and Michele Lucente, Solar γ rays as a complementary probe of dark matter, Phys. Rev. D **96**, 063010 (2017).
[122] A. Albert, R. Alfaro, C. Alvarez, R. Arceo, J. C. Arteaga-Velázquez, D. Avila Rojas, H. A. Ayala Solares, E. Belmont-Moreno, S. Y. BenZvi, C. Brisbois *et al.*, Constraints on spin-dependent dark matter scattering with long-lived mediators from TeV observations of the Sun with HAWC, Phys. Rev. D **98**, 123012 (2018).
[123] M. U. Nisa, J. F. Beacom, S. Y. BenZvi, R. K. Leane, T. Linden, K. C. Y. Ng, A. H. G. Peter, and B. Zhou, The Sun at GeV–TeV energies: A new laboratory for astroparticle physics, arXiv:1903.06349.
[124] Carl Niblaeus, Ankit Beniwal, and Joakim Edsjö, Neutrinos and gamma rays from long-lived mediator decays in the Sun, J. Cosmol. Astropart. Phys. 11 (2019) 011.
[125] A. Cuoco, P. De La Torre Luque, F. Gargano, M. Gustafsson, F. Loparco, M. N. Mazziotta, and D. Serini, Search for dark matter cosmic-ray electrons and positrons from the Sun with the Fermi Large Area Telescope, Phys. Rev. D **101**, 022002 (2020).
[126] Davide Serini, Francesco Loparco, and Mario Nicola Mazziotta, Constraints on dark matter scattering with long-lived mediators using gamma-rays from the Sun, Proc. Sci. ICRC2019 (**2019**) 544.
[127] M. N. Mazziotta, F. Loparco, D. Serini, A. Cuoco, P. De La Torre Luque, F. Gargano, and M. Gustafsson, Search for dark matter signatures in the gamma-ray emission towards the Sun with the Fermi Large Area Telescope, Phys. Rev. D **102**, 022003 (2020).
[128] Nicole F. Bell, James B. Dent, and Isaac W. Sanderson, Solar gamma ray constraints on dark matter annihilation to secluded mediators, Phys. Rev. D **104**, 023024 (2021).
[129] Raghuveer Garani and Sergio Palomares-Ruiz, Evaporation of dark matter from celestial bodies, J. Cosmol. Astropart. Phys. 05 (2022) 042.